EMBRY-RIDDLE
Aeronautical University™
SCHOLARLY COMMONS

Publications

Time-resolved Ducting of Atmospheric Acoustic-gravity Waves by Analysis of the Vertical Energy Flux

Yonghui Yu
Embry-Riddle Aeronautical University

Michael P. Hickey Ph.D.
Embry-Riddle Aeronautical University, hicke0b5@erau.edu

Follow this and additional works at: https://commons.erau.edu/publication

Part of the Atmospheric Sciences Commons

Scholarly Commons Citation

Yu, Y., and M. P. Hickey (2007), Time-resolved ducting of atmospheric acoustic-gravity waves by analysis of the vertical energy flux, Geophys. Res. Lett., 34, L02821, doi: https://doi.org/10.1029/2006GL028299

Time-resolved ducting of atmospheric acoustic-gravity waves by analysis of the vertical energy flux

Yonghui Yu[1,2] and Michael P. Hickey[1,2]

[1]   A new 2-D time-dependent model is used to simulate the propagation of an acoustic-gravity wave packet in the atmosphere. A Gaussian tropospheric heat source is assumed with a forcing period of 6.276 minutes. The atmospheric thermal structure creates three discrete wave ducts in the stratosphere, mesosphere, and lower thermosphere, respectively. The horizontally averaged vertical energy flux is derived over altitude and time in order to examine the time-resolved ducting. This ducting is characterized by alternating upward and downward energy fluxes within a particular duct, which clearly show the reflections occurring from the duct boundaries. These ducting simulations are the first that resolve the time-dependent vertical energy flux. They suggest that when ducted gravity waves are observed in the mesosphere they may also be observable at greater distances in the stratosphere. **Citation:** Yu, Y., and M. P. Hickey (2007), Time-resolved ducting of atmospheric acoustic-gravity waves by analysis of the vertical energy flux, *Geophys. Res. Lett.*, *34*, L02821, doi:10.1029/2006GL028299.

1. Introduction

[2]   Gravity waves propagating upward through the atmosphere are strongly influenced by the mean thermal structure. Thermal ducting may occur in a region of local maximum in the Brunt-Väisälä frequency, particularly for shorter period gravity waves. In this instance a region of internal wave propagation (the duct) is sandwiched between regions of evanescence. Observations of wave events in the nightglow and theoretical analysis confirm that atmospheric gravity waves may be ducted in the lower thermospheric thermal duct [*Tuan and Tadic*, 1982; *Hines and Tarasick*, 1994; *Taylor et al.*, 1995; *Isler et al.*, 1997; *Hecht et al.*, 2001; *Hickey*, 2001; *Walterscheid et al.*, 1999, 2001; *Snively and Pasko*, 2003; Y. Yu and M. P. Hickey, Numerical modeling of a gravity wave packet ducted by the thermal structure of the atmosphere, submitted to *Journal of Geophysical Research*, hereinafter referred to as Yu and Hickey, submitted manuscript, 2006a]. In addition to the mean thermal structure, winds may also play a significant role in wave ducting [*Isler et al.*, 1997; *Walterscheid et al.*, 1999; *Hecht et al.*, 2001; *Hickey*, 2001].

[3]   *Walterscheid et al.* [1999] interpreted quasi-monochromatic (QM) waves seen in airglow images as ducted or trapped waves in the lower thermospheric thermal duct. Coherent periodic structures of observed QM waves were shown by *Hecht et al.* [2001] to propagate horizontally across airglow images. Those QM waves typically had horizontal wavelengths of tens of kilometers and periods of several minutes. A numerical simulation of ducted waves requires information regarding the directions of wave propagation, the wave intrinsic periods, and their horizontal wavelengths. The intrinsic wave period is a wave parameter that varies with height in the real atmosphere due to the effects of mean winds. Because these mean winds affect wave ducting, we have chosen to deliberately exclude their effects so that we can focus on the thermal ducting alone.

[4]   In the past several authors have modeled gravity wave ducting. *Fritts and Yuan* [1989] studied wave ducting with 1-D Taylor-Goldstein solutions. *Walterscheid et al.* [2001] simulated thermal ducting above a convective storm with 2-D cylindrical coordinates. *Hickey* [2001] simulated steady-state gravity wave ducting and the airglow response to the waves using a full-wave model. *Snively* [2003] used a 2-D model to simulate ducted waves in the far-field lower thermospheric thermal duct excited by linear tropospheric forcing, and also by nonlinear breaking of tropospherically generated waves [*Snively and Pasko*, 2003]. Although inspired by previous studies, the present study uses a distinctive, nonlinear 2-D model (AGE-TIP in the works by Yu and Hickey (submitted manuscript, 2006a) and Y. Yu and M. P. Hickey (A numerical model characterizing internal gravity wave propagation into the upper atmosphere, submitted to *Journal of Geophysical Research*, 2006b, hereinafter referred to as Yu and Hickey, submitted manuscript, 2006b)) to elucidate the wave ducting by examining its vertical energy flux $\overline{p'w'}$. The basic theory of wave ducting in the atmosphere is discussed in section 2, while the model and results are presented in section 3. A discussion (section 4) and conclusion (section 5) follow.

2. Theory

[5]   In a windless atmosphere the dispersion relation given by *Hines* [1960] can be solved for the vertical wave number squared (m^2) which is then given by

$$m^2 = \frac{(N^2 - \omega^2)}{\omega^2} k^2 + \frac{(\omega^2 - \omega_a^2)}{C^2}, \qquad (1)$$

where ω is the observed frequency, C is the sound speed, N is the Brunt-Väisälä frequency, ω_a is the acoustic-cutoff frequency, and k is the horizontal wave number. The existence of thermal gradients implies that N varies with altitude, which introduces the possibility of ducting. A thermally ducted wave will be internal ($m^2 > 0$) in the region

[1]Department of Physical Sciences, Embry-Riddle Aeronautical University, Daytona Beach, Florida, USA.
[2]Department of Physics, University of Central Florida, Orlando, Florida, USA.
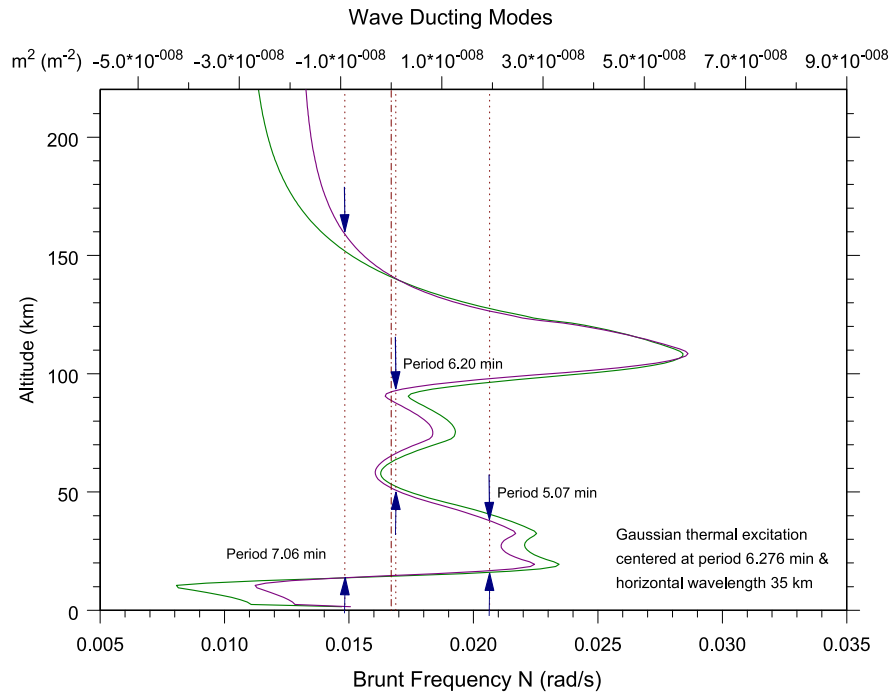
Wave Ducting Modes

Figure 1. The Brunt frequency N (units in rad s^{-1}, green line, lower x-axis) and the m^2 profile (units in m^{-2}, magenta line, upper x-axis) of the primary wave (period 6.276 min, λ_h = 35 km). The three vertical lines (red, dot-dot) identify waves of period 7.06, 6.20, and 5.07 min. Three pairs of blue arrows identify three individual ducts. The vertical line (red, dash-dot) signifies m = 0 at a period of 6.276 min.

near a local maximum of N, and become evanescent ($m^2 < 0$) at some vertical distances either side of this where N has decreased [*Hines*, 1960; *Walterscheid et al.*, 1999; *Hecht et al.*, 2001; *Hickey*, 2001].

[6] Alternatively, a gravity wave may be ducted between the ground and some higher altitude where the wave becomes locally evanescent [*Tuan and Tadic*, 1982]. However, while these are necessary conditions for wave ducting, they are not sufficient conditions. Whether or not wave ducting is strong or leaky depends on the distance between the duct boundaries and the vertical structure of the wave. Perfect thermal ducting requires that an integer number of half vertical wavelengths fits exactly in the internal wave region ($m^2 > 0$), so the vertical energy flux could approach zero at the duct boundaries and strong standing wave behavior will result [*Hickey*, 2001; *Walterscheid et al.*, 2001]. Another condition required for strong ducting is that the evanescent regions below and above the duct are thick enough to efficiently reflect the ducted waves. Therefore, only certain combinations of wave period and horizontal wavelength favor strong ducting in atmospheric thermal ducts.

3. Results

[7] The current study of thermal ducting is implemented with the 2-D AGE-TIP model described in detail elsewhere (Yu and Hickey, submitted manuscript, 2006b). Briefly, the model solves the Navier-Stokes equations including eddy and molecular processes using a time-splitting technique involving Lax-Wendroff and Newton-Raphson schemes. A sponge layer is applied at the model upper boundary, and periodic boundary conditions are applied at the lateral

boundaries (separated by one horizontal wavelength) to simulate a horizontally infinite domain. The horizontal and vertical grid spacings are 0.5 km and 1.0 km, respectively. The time step used is 0.7 sec. The atmospheric mean state was specified by using the MSIS-E-90 model [*Hedin*, 1991] for 1993 Jan 15, 18.5°N latitude and 0.0° longitude, local time 2200 hrs. The solar and geomagnetic indices were $F_{10.7}$ = $F_{10.7A}$ = 87 and a_p = 12 for moderately disturbed conditions. Mean winds were excluded from this analysis. A full-wave model was first used to determine the parameters of a strongly ducted gravity wave in the lower thermospheric thermal duct [*Hickey*, 2001; Yu and Hickey, submitted manuscript, 2006a]. This analysis produced a wave period of 6.276 min, a horizontal wavelength of 35.0 km, and a horizontal phase speed of 92.95 m s^{-1}. They are used to excite a gravity wave packet thermally forced in the troposphere. The thermal excitation Q_w (K s^{-1}) is prescribed by the following equation

$$Q_w(x, z, t) = 10^{-5} \exp\left(-(t - \tau)^2/2\Delta t^2\right)$$
$$\cdot \exp\left(-(z - \xi)^2/2\Delta z^2\right) \sin(k_0 x - \omega_0 t), \qquad (2)$$

where Δz = 0.8 km, ξ = 8 km, Δt = 6.276 min, and τ = 37.656 min. The forcing frequency and horizontal wave number are given by $\omega_0 = 2\pi/6.276$ min and $k_0 = 2\pi/35$ km, respectively. The magnitude of the excitation is chosen to be small so that the resulting gravity wave amplitudes remain small and linear at all altitudes. Note that this excitation is similar in a form to that of *Snively and Pasko* [2003], but theirs appears in the vertical momentum equation as a mechanical standing wave oscillator.
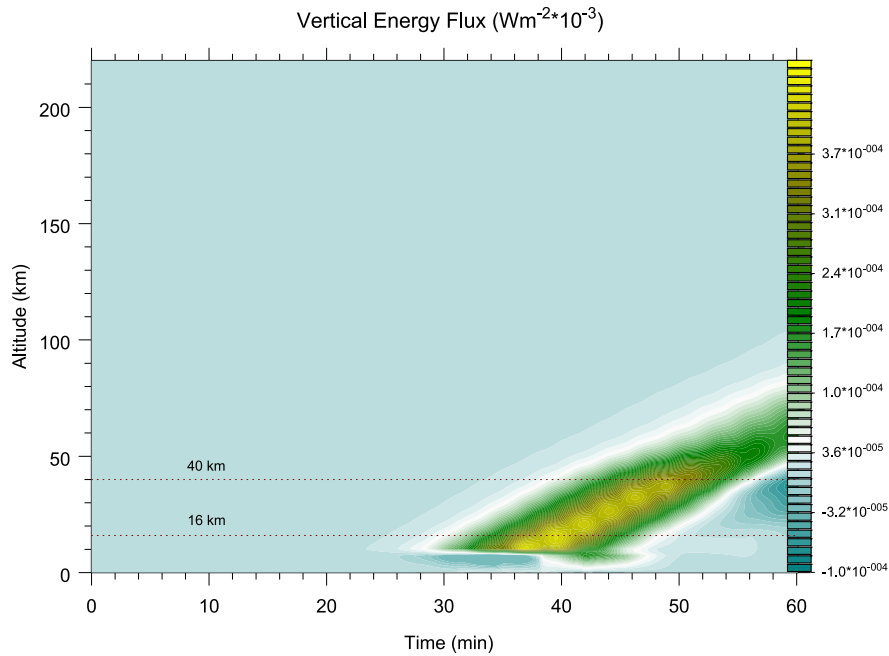
Vertical Energy Flux (Wm^{-2}*10^{-3})

Figure 2. Vertical energy flux (W m^{-2}) during the 1st hour of simulation.

[8] The height variation of the Brunt-Väisälä frequency N is shown in Figure 1. Also shown are three ducting regions and the associated ducted waves for the horizontal wavelength of 35 km. The stratospheric duct is estimated to lie between ∼16 and ∼40 km, and the mesospheric duct is between ∼52.5 and ∼91.5 km. The periods of the ducted wave modes identified in Figure 1 were determined through a spectral analysis of time series of resulting wave fields, as described in more detail by Yu and Hickey (submitted manuscript, 2006a). The stratospheric duct supports a wave mode of period 5.07 min, the duct between the lower thermosphere and the tropopause supports a wave mode of period 7.06 min, and the mesosphere and lower thermosphere (MLT) duct supports a wave mode of period 6.20 min (Yu and Hickey, submitted manuscript, 2006a). Figure 1 also shows the square of the vertical wave number, m^2, calculated for the primary period of 6.276 min. For this wave m^2 is negative in several regions, which implies that the wave is evanescent there. The wave is evanescent below ∼15 km altitude, over a 10 km region centered near 55 km
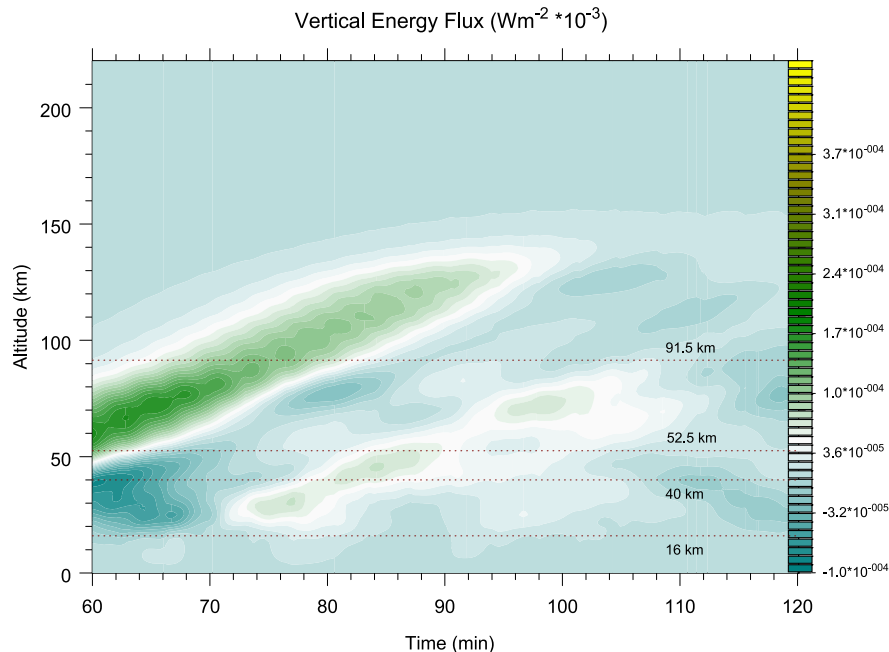
Vertical Energy Flux (Wm^{-2} *10^{-3})

Figure 3. Vertical energy flux (W m^{-2}) during the 2nd hour of simulation.
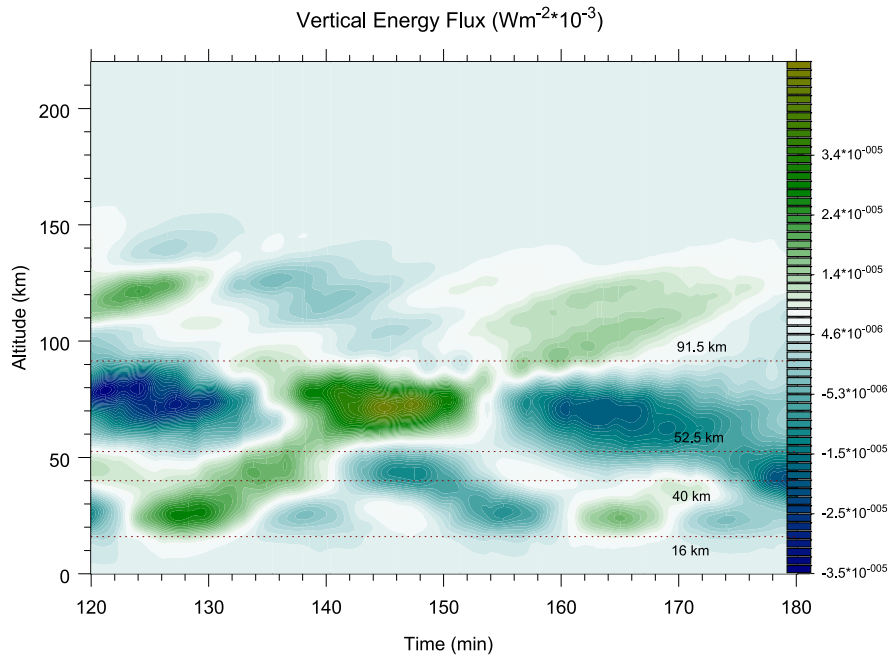
Figure 4. Vertical energy flux (W m^{-2}) during the 3rd hour of simulation.

altitude, over a 3 km region centered near 90 km altitude, and above $\sim$140 km altitude. Therefore, this wave can be ducted in three different internal wave regions lying between these evanescent regions.

[9] The horizontally averaged vertical energy flux, $\overline{p'w'}$ is shown as a function of height and time in Figures 2–5. Note that the scaling in Figures 2–5 is not identical. Figures 2 and 3 share the same scaling, while Figures 4 and 5 share a different scaling.

[10] The strongest wave forcing occurs in the first hour of the simulation in the troposphere near 38 min (Figure 2). The maximum upward energy flux is $\sim$5.0 $\times$ 10^{-7} W m^{-2}. Prior to 38 min the energy flux is positive (upward) above the source, and negative (downward) below the source. Below the source region and for times 38 min $\leq$ t $\leq$ 48 min, the direction of the energy flux changes to upward after reflecting from the ground. Above the source the energy flux remains positive for times less than 50 min, while for subsequent times a weaker downward energy flux is evident,
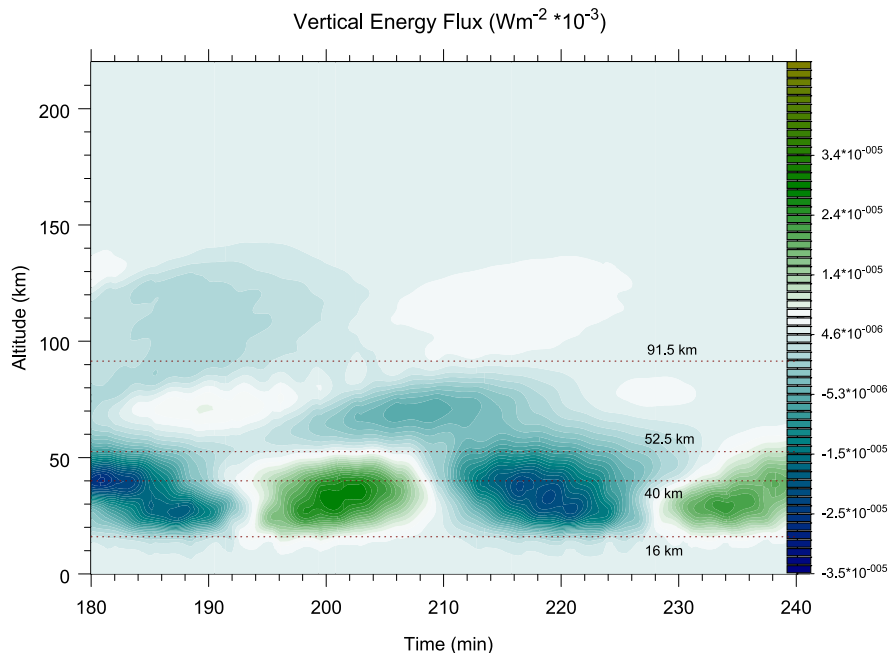

Figure 5. Vertical energy flux (W m^{-2}) during the 4th hour of simulation.

which becomes especially noticeable near 1 hr and $z = 30$ km. The downward directed energy flux is a consequence of partial reflections due to evanescence of the high frequency ($\tau \sim 5$ min) component of the wave packet, which is associated with the height variation of the N or m^2 shown in Figure 1. It is also evident that the upward energy flux remains approximately constant up to ~ 40 km altitude, after which it decreases due to partial reflections and propagation through the evanescent region. The energy flux that remains directed upward from the source in Figure 2 has a vertical group velocity of ~ 42.3 m s^{-1}. By comparison, using the forcing frequency, wave number and the mean state parameters at 30 km altitude in equation (1) yields a vertical group velocity ($\partial \omega / \partial m$) of ~ 42.4 m s^{-1}.

[11] Figure 3 shows the wave vertical energy flux for the second hour of the simulation. The main wave packet continues propagating upward into the thermosphere with a vertical group velocity of ~ 32.2 m s^{-1}, which is smaller than the value given above for the lower part of the atmosphere (Figure 2). There are two reasons for this. First, spectral analysis (Yu and Hickey, submitted manuscript, 2006a, Figure 5) confirms that some of the higher frequency (and faster) components of the wave packet are reflected in the upper stratosphere, impeding their propagation to greater altitudes. Second, the mean atmospheric stability (N) is lower in the mesosphere, which reduces the vertical wave numbers of the waves thereby reducing the vertical group velocity. The results shown in Figure 3 also clearly indicate that the downward reflected part of the packet tends to remain in the stratospheric duct. At later times (~ 70 min) this trapped wave is reflected upward and continues propagating upward until a time of ~ 90 min. Weak partial reflections of this part of the packet subsequently occur, with some upward (and weaker) penetration into the mesosphere at times greater than 90 min. The primary upward propagating packet weakens as it approaches the thermosphere, primarily as a consequence of partial reflections occurring in the mesopause region. Wave trapping is evident in the mesosphere centered at ~ 75 km altitude, with a maximum energy flux occurring at a time of 100 min and minima occurring at times of 80 and 120 min. Assuming a vertical group velocity of ~ 32.2 m s^{-1} for the wave packet in this region of the atmosphere leads to an estimated duct depth of ~ 38.6 km. This value compares favorably with the result shown in Figure 1 of this paper (~ 39.0 km) for this region of the atmosphere.

[12] Figures 4 and 5 show the vertical energy flux plotted on a magnified scale to more clearly reveal the long-term behavior of the wave ducting. The results shown in Figure 4 reveal ducting occurring in the stratosphere (~ 30 km) and in the mesosphere (~ 75 km), identified by the alternating direction of the vertical energy flux within each of the ducts. In the mesospheric duct the alternating motion occurs with a period of ~ 40 min while in the stratospheric duct it occurs with a period of ~ 20 min for times between ~ 2 and 3 hrs (Figure 4), and of ~ 40 min for times beyond 3 hrs (Figure 5). The results in Figure 4 also show that the thin evanescent region near 90 km altitude (see Figure 1 too) is strong enough to support ducting below (in the mesosphere) and above (in the lower thermosphere). At longer times in the simulation (beyond 3 hrs, Figure 5) most signs of MLT wave ducting have largely disappeared, but stratospheric

ducting persists at least out to 4 hrs. The waves ducted in the stratosphere at times between 2 and 3 hrs dissipate and weaken (compare the energy flux at ~ 128 min with that at ~ 165 min). Wave energy in the MLT duct begins descending into the stratospheric duct at ~ 170 min. At subsequent times the ducting strengthens in the stratospheric duct and the energy flux exhibits a similar characteristic period (~ 40 min), as the "precursor" MLT region ducted waves. We believe that during this time period the waves ducted in the stratosphere originated from the overlying MLT region. We base this on two observations. First, the energy flux associated with the waves ducted in the stratosphere displays the same 40 min period variations as those of the mesosphere. Second, the energy flux mentioned above strengthens during the fourth hour, which can only occur by energy entering the duct. Note, however that after the first three hours in the simulation the slower waves reflecting from the overlying MLT region superimpose on the faster waves initially trapped in the stratospheric duct. At very long times (>4 hrs) our simulations (not shown) reveal that wave energy leaks upward from the stratospheric duct to the MLT region. However, the energy of these waves is considerably reduced and is very small ($\sim 10^{-8}$ W m^{-2}).

4. Discussion

[13] The shorter period waves considered here are all confined to the atmospheric region below ~ 150 km altitude due to evanescence at greater altitudes and associated reflections. The fast waves reach the thermosphere quickly (taking less than ~ 90 min), but they suffer partial reflections at all heights along the way. The downward propagating wave energy is subsequently trapped at lower levels where it resides in two main ducts, one in the mesosphere and the other in the stratosphere. The ducting in the stratosphere is the most persistent, with significant energy remaining trapped there for times of ~ 4 hrs.

[14] In Figure 4 a clear ducting signature was seen between altitudes of ~ 52.5 km and ~ 91.5 km identified by the alternating direction of the vertical energy flux. The thin evanescent region near 90 km altitude, identified by the thin horizontal line in Figure 4, causes partial reflection, while also allowing partial transmission of wave energy. The energy flux is zero in the 90 km region. Although the typical periods of the individual waves within the packet are short and of several minutes, the energy flux associated with trapped packet motions exhibits much longer periods of ~ 40 min in the mesosphere (Figure 4), and also in the stratosphere (Figure 5). This behavior can be explained by non-ideal ducting in which cancellation between upward and downward waves is incomplete. It raises the possibility that measurements of low temporal resolution (below the Nyquist frequency) could be misinterpreted in terms of long period motions.

[15] We have focused our attention on the energy flux, but we note that this is not a wave diagnostic variable that can be easily measured. In contrast, the wave-associated momentum flux is commonly estimated from radar and lidar observations of horizontal and vertical velocities, and also from airglow imaging measurements [*Gardner et al.*, 1999]. The momentum flux derived from our simulations (not shown) behaves similar to the vertical energy flux. Our

findings will apply equally well to the momentum flux and can, in principle, be observationally confirmed.

[16] Although this paper has focused on the vertical energy flux it should be recognized that the waves also have an associated horizontal energy flux. Our simulations reveal that the horizontal energy flux (not shown) has a one-to-one correlation with the vertical energy flux, and both are approximately zero at the duct boundaries. For perfectly ducted waves we expect perfect cancellation of the upward and downward energy fluxes so that the vertical energy flux within such a duct would be zero (but the horizontal energy flux would be non-zero). However, our wave train is too short to fill the entire vertical extent of the atmosphere because our source generates a Gaussian wave packet and therefore we never generate fully ducted modes. Airglow imagers frequently observe coherent monochromatic structures in the mesopause region that can be followed as they propagate across the field of view (typically ~200 km), which implies that many "bounces" must be occurring (see the discussion by *Hecht et al.* [2001]). These are usually "far-field" observations, so interference effects associated with freely propagating waves or waves ducted in other atmospheric regions are usually unimportant.

[17] *Walterscheid et al.* [2001] used a model with cylindrical symmetry to simulate acoustic-gravity waves generated by a convective source due to the latent heat release from rainfall associated with a Hector event in northern Australia. They also examined the effect of using different source characteristics and found that a quasi-monochromatic (QM) source generated ducted waves that were similar to those of the more realistic Hector forcing. Notable differences included a stronger standing wave behavior and less weakening with radial propagation distances associated with the QM source. Because in our simulations the tropospheric wave forcing was characterized by a monochromatic variation of fixed horizontal wavelength and period modulated by a Gaussian variation in time, the results of *Walterscheid et al.* [2001] suggest that we may be overestimating the strength of the ducting in our simulations.

[18] Winds have a significant effect on gravity wave propagation in the atmosphere but we have neglected them here in order to focus on the thermal ducting. Strong wind shears will alter the details of the ducting by impacting the wave parameters (wave period and vertical wave number) that satisfy the ducting criteria. Numerical simulations including the effects of mean winds that include shears have been discussed by *Hecht et al.* [2001]. We know that ducting occurs in spite of mean winds because ducted waves are fairly common occurrences in airglow observations. Later we will perform a detailed study including mean winds and shears.

5. Conclusion

[19] We have used a new time-dependent model to simulate the propagation of a wave packet from the troposphere into the overlying atmosphere. By examining the horizontally averaged vertical energy flux we have elucidated the coupling of wave energy between different atmospheric regions and also revealed the trapping of wave energy in various atmospheric ducts. Although the waves we have studied are all of short period (~6 min), the energy flux exhibits longer period (~20 min and ~40 min) behavior associated with the time taken for the waves to travel between the lower and upper duct boundaries. Ducting persists in the mesospheric duct till ~3 hrs and in the stratospheric duct till ~4 hrs. Eventually (for times > 4 hrs) the waves in the stratospheric duct leak upward to the mesosphere, but the relatively small amount of wave energy would likely make the waves unobservable. Our findings should apply equally well to the momentum flux and so can be observationally confirmed. Our simulations suggest that when ducted gravity waves are observed in the mesosphere they may also be observable at greater distances in the stratosphere.

References

Fritts, D. C., and L. Yuan (1989), An analysis of gravity wave ducting in the atmosphere: Eckart's resonances in thermal and Doppler ducts, *J. Geophys. Res.*, *94*(D15), 18,455–18,466.

Gardner, C. S., K. Gulati, Y. Zhao, and G. Swenson (1999), Measuring gravity wave momentum fluxes with airglow imagers, *J. Geophys. Res.*, *104*(D10), 11,903–11,916.

Hecht, J. H., R. L. Walterscheid, M. P. Hickey, and S. J. Franke (2001), Climatology and modeling of quasi-monochromatic atmospheric gravity waves observed over Urbana, Illinois, *J. Geophys. Res.*, *106*(D6), 5181–5196.

Hedin, A. E. (1991), Extension of the MSIS thermosphere model into the middle and lower atmosphere, *J. Geophys. Res.*, *96*(A2), 1159–1172.

Hickey, M. P. (2001), Airglow variations associated with nonideal ducting of gravity waves in the lower thermosphere region, *J. Geophys. Res.*, *106*(D16), 17,907–17,918.

Hines, C. O. (1960), Internal atmospheric gravity waves at ionospheric heights, *Can. J. Phys.*, *38*, 1441–1481.

Hines, C. O., and D. W. Tarasick (1994), Airglow response to vertically standing gravity waves, *Geophys. Res. Lett.*, *21*(24), 2729–2732.

Isler, J. R., M. J. Taylor, and D. C. Fritts (1997), Observational evidence of wave ducting and evanescence in the mesosphere, *J. Geophys. Res.*, *102*(D22), 26,301–26,313.

Snively, J. B. (2003), Tropospheric forcing as a source of quasi-monochromatic short-period gravity waves observed in the upper mesosphere and lower thermosphere, M. S. thesis, Penn State Univ., University Park.

Snively, J. B., and V. P. Pasko (2003), Breaking of thunderstorm-generated gravity waves as a source of short-period ducted waves at mesopause altitudes, *Geophys. Res. Lett.*, *30*(24), 2254, doi:10.1029/2003GL018436.

Taylor, M. J., M. B. Bishop, and V. Taylor (1995), All-sky measurements of short period waves imaged in the OI (557.7 nm), Na (589.2 nm) and near infrared OH and O$_2$ (0, 1) nightglow emissions during the ALOHA-93 campaign, *Geophys. Res. Lett.*, *22*(20), 2833–2836.

Tuan, T.-F., and D. Tadic (1982), A dispersion formula for analyzing "model interference" among guided and free gravity wave modes and other phenomena in a realistic atmosphere, *J. Geophys. Res.*, *87*, 1648–1668.

Walterscheid, R. L., J. H. Hecht, R. A. Vincent, I. M. Reid, J. Woithe, and M. P. Hickey (1999), Analysis and interpretation of airglow and radar observations of quasi-monochromatic gravity waves in the upper mesosphere and lower thermosphere over Adelaide, Australia (35°S, 138°E), *J. Atmos. Sol. Terr. Phys.*, *61*, 461–478.

Walterscheid, R. L., G. Schubert, and D. G. Brinkman (2001), Small-scale gravity waves in the upper mesosphere and lower thermosphere generated by deep tropical convection, *J. Geophys. Res.*, *106*(D23), 31,825–31,832.

_____

M. P. Hickey and Y. Yu, Department of Physical Sciences, Embry-Riddle Aeronautical University, Daytona Beach, FL 32114, USA. (michael.hickey@erau.edu; yonghui.yu@erau.edu)